

Anomaly Detection based on Markov Data: A Statistical Depth Approach

Carlos Fernández^{1[0000-0002-8577-865X]} and Stephan
Cléménçon^{1[0000-0002-5879-9500]}

LTCI, Télécom Paris, Institut Polytechnique de Paris
`{fernandez,stephan.clemencon}@telecom-paris.fr`

Abstract. The purpose of this article is to extend the notion of statistical depth to the case of sample paths of a Markov chain. Initially introduced to define a center-outward ordering of points in the support of a multivariate distribution, depth functions permit to generalize the notions of quantiles and (signed) ranks for observations in \mathbb{R}^d with $d > 1$, as well as statistical procedures based on such quantities. Here we develop a general theoretical framework for evaluating the depth of a Markov sample path and recovering it statistically from an estimate of its transition probability with (non-) asymptotic guarantees. We also detail some of its applications, focusing particularly on unsupervised anomaly detection. Beyond the theoretical analysis carried out, numerical experiments are displayed, providing empirical evidence of the relevance of the novel concept we introduce here to quantify the degree of abnormality of Markov paths of variable length.

Keywords: Anomaly detection · Statistical Depth · Markov chains

1 Introduction

The concept of Markov chain provides a very popular time-series model, ubiquitous in applications (*e.g.* systems engineering, bioinformatics, mathematical finance, operations research) to describe the dynamics governing the evolution of random time phenomena in a parsimonious way, namely systems with a past, whose future distribution depends on the most recent part only.

This paper is devoted to the extension of the *statistical depth* concept, originally introduced in [49] to overcome the lack of natural order on \mathbb{R}^d for $d \geq 2$, to sample paths with variable length of a Markov chain $\mathbf{X} = (X_n)_{n \in \mathbb{N}}$. Whereas recent alternative approaches for curve/functional data are essentially based on topological/metric properties of the path space (see *e.g.* [46,23]) and generally produce too large quantile regions when applied to Markov data as will be shown later, the framework we develop is tailored to the Markov setting. It is based on the description of the law of a Markov chain by its transition probability kernel and can be considered as a very natural extension of the multivariate case. Given a statistical depth on the state space, we propose to define the depth of a sample path as the geometric average of the depth of each state involved in it w.r.t. the

transition probability evaluated at the preceding state. We show that the depth on the torus of all finite length trajectories thus constructed inherits many of the properties that the multivariate depth may enjoy, has significant computational advantages compared to its competitors and can be interpreted in a very intuitive fashion: the greater the average number of deep transitions, the deeper the path. The accuracy of sampling versions of the Markov depth promoted is rigorously established in the form of (non-) asymptotic upper confidence bounds in the spirit of generalization guarantees in statistical learning theory. While such results like ours have been mainly established in the i.i.d. case (see *e.g.* [14]), the case of observations with a dependency structure, time-series in particular, has been the subject of intensive study in recent years, see for instance [1], [2], [47], [11] [48], [29] or [15]. These results mainly rely on extensions of probabilistic bounds for uniform deviations of i.i.d. averages from their expectation to the case of *weakly dependent training data*, under general assumptions related to the decay rate of *mixing coefficients*, see [43]. However, few works, with the exception of [11] for instance, are specific to the case of Markov chains and exploit their specific dynamics as we do in this paper.

Several promising applications related to the statistical analysis of Markov paths of variable lengths are also discussed. Motivated by practical problems in various domains (*e.g.* health monitoring, quality control, security), we pay particular attention to the task of detecting abnormal trajectories. In the numerical experiments that have been carried out, the proposed methodology performs significantly better than pre-existing approaches, paving the way for its use in a wider range of tasks.

The paper is structured as follows. In section 2, the main notions of statistical depth are briefly recalled alongside basic elements of Markov chain theory. In section 3 we introduce the concept of *Markovian depth function*, we explain how to construct Markovian depth functions based on statistical depths defined on the state space and we study its main properties. Various numerical experiments illustrating the relevance of the concept we propose are presented in section 4. Section 5 collects a few concluding remarks and perspectives for further research, while, due to space limitations, all technical proofs as well as additional discussions, examples and applications are postponed to the Appendix.

2 Background and Preliminaries

As a first go, we briefly recall some basic notions pertaining to statistical depth theory and key concepts in the study of Markov chains (refer to *e.g.* [36,18] for a more detailed account), which shall be used in the paper. Throughout the article, we denote by $\mathbb{I}\{B\}$ the indicator function of any event B , by δ_a the Dirac mass at any point a and by \Rightarrow convergence in distribution. The Euclidean inner product and norm on \mathbb{R}^d are denoted by $\langle \cdot, \cdot \rangle$ and $\|\cdot\|$.

2.1 Statistical Depth

Given the lack of any “natural order” on \mathbb{R}^d when $d \geq 2$, the notion of *statistical depth* allows to define a center-outward ordering of points in the support of a probability distribution P on \mathbb{R}^d and, as a result, to extend the notions of order and (signed) rank statistics to multivariate data, see [37]. By *depth function* relative to P is meant a function that determines the centrality of any point $x \in \mathbb{R}^d$ with respect to the probability measure P , that is to say any bounded non-negative Borel-measurable function $D_P : \mathbb{R}^d \rightarrow \mathbb{R}_+$ such that the points $x \in \mathbb{R}^d$ near the ‘center’ of the mass are the deepest (*i.e.* such that $D_P(x)$ is among the highest values taken by the function). The depth D_P thus enables us to define a preorder for multivariate points $x \in \mathbb{R}^d$. Originally introduced in the seminal contribution [49], the *half-space depth* of x in \mathbb{R}^d relative to P is the minimum of the measure $P(\mathcal{H})$ taken over all closed half-spaces $\mathcal{H} \subset \mathbb{R}^d$ such that $x \in \mathcal{H}$. Many alternatives have been developed, see *e.g.* [32], [35], [39], [13] or [9] among others. Refer to A1 in the Appendix for a list of popular statistical depths for multivariate distributions and a discussion about computational issues. In [51], an axiomatic nomenclature of statistical depths has been devised, providing a systematic way of comparing their merits and drawbacks. Precisely, the four properties below should be ideally satisfied for any distribution on \mathbb{R}^d .

- (P1) (AFFINE INVARIANCE) Meaning by P_X the law of any r.v. X valued in \mathbb{R}^d , it holds: $D_{P_{AX+b}}(Ax + b) = D_P(x)$ for all $x \in \mathbb{R}^d$, any r.v. X taking its values in \mathbb{R}^d , any $d \times d$ nonsingular matrix A with real entries and any b in \mathbb{R}^d .
- (P2) (VANISHING AT INFINITY) For any probability law P on \mathbb{R}^d , the depth function D_P vanishes at infinity, *i.e.* $D_P(x) \rightarrow 0$ as $\|x\|$ tends to infinity.
- (P3) (MAXIMALITY AT CENTER) For any probability distribution P on \mathbb{R}^d possessing a symmetry center x_P (in a sense to be specified), the depth function D_P takes its maximum value at it, *i.e.* $D_P(x_P) = \sup_{x \in \mathbb{R}^d} D_P(x)$.
- (P4) (MONOTONICITY RELATIVE TO THE DEEPEST POINT) For any distribution P on \mathbb{R}^d with deepest point x_P , the depth at any point x in \mathbb{R}^d decreases as one moves away from x_P along any ray passing through it, *i.e.* $D_P(x) \leq D_P(x_P + \alpha(x - x_P))$ for any α in $[0, 1]$.

Several studies have examined whether some of the properties listed above are verified by the various notions of statistical depth proposed in the literature, see *e.g.* [51]. The continuity properties of the depths, in both x and P , have also been studied for most statistical depths, see *e.g.* [16,41]. As the distribution P of interest is usually unknown in practice, its analysis must rely on the observation of $N \geq 1$ independent realizations X_1, \dots, X_N of P . A statistical version of $D_P(x)$ can be built by replacing P with an empirical counterpart \hat{P}_N based on the X_i ’s, *e.g.* the raw empirical distribution $(1/N) \sum_{i=1}^N \delta_{X_i}$, to get the *empirical depth function* $D_{\hat{P}_N}(x)$. The consistency and asymptotic normality of empirical depth functions have been analyzed for different notions of statistical depth [16], and concentration results for empirical half-space depth and contours can be found in [8]. The ranks and order statistics derived from a depth function can be

used for a variety of tasks, *e.g.* classification and clustering [27], anomaly detection [39] or two-sample tests [45] among others. The case of functional data has received some attention in the literature. Although most practical approaches consist in projecting first the functional data onto an appropriate finite dimensional space (*filtering*) and using next a notion of multivariate depth, certain methods recently documented rely on metrics or exploit the geometry of the trajectories/curves in the path space, see [46]. As we will see in the following, such techniques perform poorly when applied to Markov data, given the possibly great dispersion of Markov probability laws. In contrast to the methodology we propose, none of them exploits the underlying Markov dynamics/structure of paths and is suitable to analyze trajectories of different lengths.

2.2 Basic Properties of Markov Chains

We first recall a few definitions concerning the communication structure and the stochastic stability of Markov chains. Let $\mathbf{X} = (X_n)_{n \in \mathbb{N}}$ be a (time-homogeneous) chain (of order 1) defined on some probability space $(\Omega, \mathcal{F}, \mathbb{P})$ with a countably generated state space $E \subseteq \mathbb{R}^d$ equipped with its Borel σ -field $\mathcal{B}(E)$, transition probability kernel $\Pi : (x, A) \in E \times \mathcal{B}(E) \mapsto \Pi_x(A)$ and initial probability distribution ν . For any $A \in \mathcal{B}(E)$ and $n \in \mathbb{N}$, we thus have that $X_0 \sim \nu$ and

$$\mathbb{P}(X_{n+1} \in A \mid X_0, \dots, X_n) = \Pi_{X_n}(A) \quad a.s. \quad (1)$$

We denote by \mathbb{P}_ν (respectively, by \mathbb{P}_x for x in E) the probability measure on the underlying probability space such that $X_0 \sim \nu$ (resp. $X_0 = x$) and by $\mathbb{E}_\nu[\cdot]$ the \mathbb{P}_ν -expectation (resp. by $\mathbb{E}_x[\cdot]$ the \mathbb{P}_x -expectation).

The chain \mathbf{X} is said to be *irreducible* if there exists a σ -finite measure ψ s.t. for all set $B \in \mathcal{B}(E)$, when $\psi(B) > 0$, the chain visits B with strictly positive probability, no matter what the starting point is. A Borel set A is *Harris recurrent* for the chain \mathbf{X} if for any $x \in A$, $\mathbb{P}_x(\sum_{n=1}^{\infty} \mathbb{I}\{X_n \in A\} = \infty) = 1$. The chain \mathbf{X} is said *Harris recurrent* if it is ψ -irreducible and every measurable set A s.t. $\psi(A) > 0$ is Harris recurrent. When the chain is Harris recurrent, we have the property that $\mathbb{P}_x(\sum_{n=1}^{\infty} \mathbb{I}\{X_n \in A\} = \infty) = 1$ for any $x \in E$ and any $A \in \mathcal{B}(E)$ such that $\psi(A) > 0$. A probability measure μ on E is said invariant for \mathbf{X} when $\mu\Pi = \mu$, where $\mu\Pi(dy) = \int_{x \in E} \mu(dx)\Pi_x(dy)$. An irreducible chain is said *positive recurrent* when it admits an invariant probability (it is then unique).

Example 1. (MODULATED RANDOM WALK) Consider the model defined by $X_0 = x_0 \geq 0$ and $X_{n+1} = \max(0, X_n + W_n)$ for $n \in \mathbb{N}$ where (W_n) is a sequence of i.i.d. random variables with distribution F . Then, X_n is a Markov chain on $E = [0, \infty)$ with transition kernel: $\Pi(x, [0, y]) = F(y - x) \quad x, y \geq 0$. When $\mathbb{E}[W_1] < 0$, the chain is positive recurrent [36, Proposition 11.4.1]. Such a modulated random walk on the half-line models various systems, such as *content-dependent storage processes*, *work-modulated single server queues*, see *e.g.* [3, Section III.6].

Denote by $\mathbb{T} = \cup_{n \geq 1} E^n$ the torus of all trajectories of finite length in the state space E , equipped with its usual topology $\mathcal{T} = \{O \subset \mathbb{T} : \forall n \geq 1, O \cap E^n \in$

$\mathcal{B}(E^n)$ } (see [19, pp. 131] or Section A2 of the Appendix for further details). Any observed finite length path (x_0, \dots, x_n) of \mathbf{X} is an element of \mathbb{T} . Our goal is to develop tools for assessing the *centrality*, or the *outlyingness* conversely, of elements of \mathbb{T} w.r.t. the law of a chain \mathbf{X} . As illustrated in the example below, classic path depths based on the geometry of the space of trajectories are inappropriate even in the case where all trajectories have the same length.

Example 2. (LIMITS OF GEOMETRIC APPROACHES) Consider the model described in Example 1, where $W_n = -1.1 \times Y_n + 1$ and the Y_n 's are i.i.d. exponential r.v.'s with mean 1. Note that, with probability 1: $W_n \leq 1$, hence $X_{n+1} - X_n \leq 1$. Fig. 1a shows, in solid red line, an unfeasible trajectory $\mathbf{x} = (0, x_1, \dots, x_5)$ where $x_2 - x_1 = 1.1$, sandwiched between two feasible trajectories (green/orange dashed lines). We have calculated the Lens and Mahalanobis depths (MBD) of this unfeasible trajectory w.r.t. the joint probability distribution of X_1, \dots, X_5 , obtaining the values 0.42 and 0.097 respectively, very close to the depths of the feasible ones that surround it in Fig. 1b and 1c..

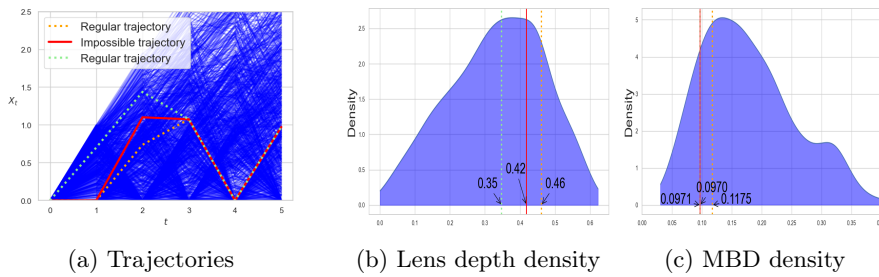


Fig. 1: (a) an unfeasible trajectory (red line) of the modulated random walk surrounded by two regular trajectories (green and orange dotted lines). (b) and (c), the densities of Lens and Mahalanobis depths w.r.t. the joint distribution of X_1, \dots, X_5 .

3 Depth functions for Markov Chains

This section is devoted to extending the concept of statistical depth function to the domain of Markov chains. We propose a very general mechanism for constructing such Markov depth functions and then investigate their main properties. Particular attention is paid to the study of sampling versions.

3.1 Markovian Depth Functions

As stated in the introduction, our goal is to extend the notion of depth function to the space \mathbb{T} of finite length trajectories of a Markov chain in order to assess the centrality or outlyingness of Markov paths. The following is a list of a priori desirable properties for such functions on \mathbb{T} .

Definition 1 (Markovian depth function). A statistical depth function w.r.t. the distribution of the Markov chain \mathbf{X} is a function $\mathbf{D}_{\mathbf{X}} : \mathbb{T} \rightarrow \mathbb{R}_+$ that may satisfy some of the following properties:

(M0) (INDEPENDENCE FROM THE INITIAL LAW) If \mathbf{X} and \mathbf{X}' are two Markov chains with the same transition kernel, then:

$$\forall \mathbf{x} \in \mathbb{T}, \quad \mathbf{D}_{\mathbf{X}}(\mathbf{x}) = \mathbf{D}_{\mathbf{X}'}(\mathbf{x}).$$

(M1) (AFFINE INVARIANCE) For any $d \times d$ non singular matrix A , $b \in \mathbb{R}^d$, it holds:

$$\forall \mathbf{x} \in \mathbb{T}, \quad \mathbf{D}_{A\mathbf{x}+b}(A\mathbf{x} + b) = \mathbf{D}_{\mathbf{X}}(\mathbf{x}),$$

where we set $A\mathbf{x} + b = (Ax_0 + b, \dots, Ax_n + b)$ when $\mathbf{x} = (x_0, \dots, x_n)$.

(M2) (VANISHING AT INFINITY) We have $\mathbf{D}_{\mathbf{X}}(\mathbf{x}) \rightarrow 0$ as \mathbf{x} “tends to infinity” in the sense of \mathbb{T} ’s topology \mathcal{T} .

Property (M0) in the above definition guarantees that the depth only depends on the dynamics, *i.e.* the transition probability kernel Π , which can be easily estimated with (non-) asymptotic guarantees based on the observation of a single Markov path of sufficiently long length $N \geq 1$ (see *e.g.* [10] and [28] and the references therein). Properties (M1) and (M2) are the natural extensions of the properties (P1) and (P2) of the depth functions on E to the path space \mathbb{T} . Regarding the extension of property (P3), though symmetry centers can be defined in the path space in certain (seldom) situations, they do not necessarily correspond to realizable paths, as illustrated in section A4 of the Supplementary Material, in which case the maximality at center property is absolutely not desirable. Notice also that, because of the absence of any vector space structure on \mathbb{T} , there is no natural equivalent to the monotonicity property (P4) in the Markovian case. In the next subsection we propose a simple way to build Markovian depth functions on \mathbb{T} based on statistical depth functions on E .

3.2 Markovian Sample Path Depth

Consider any notion of statistical depth D on E and let $\mathbf{x} = (x_0, \dots, x_n)$ be a finite length realization of the chain \mathbf{X} with initial distribution ν and kernel Π . For any $i \in \{1, \dots, n\}$, x_i is a realization of the transition probability $\Pi_{x_{i-1}}$, a distribution on E , and its depth can be naturally quantified through $D_{\Pi_{x_{i-1}}}(x_i)$. We propose to define the depth of \mathbf{x} by aggregating the depth of all transitions forming the path \mathbf{x} , as the geometric mean of the depths of each state transition.

Definition 2 (Markovian path depth). With the convention that $\sqrt[n]{0} = 0$ for $n \geq 1$, the Markov depth function of a chain \mathbf{X} with transition Π based on the multivariate statistical depth D is the real-valued function defined on the torus \mathbb{T} of all trajectories of finite length as: $\forall n \geq 1, \forall \mathbf{x} = (x_0, \dots, x_n) \in E^{n+1}$,

$$D_{\Pi}(\mathbf{x}) = \sqrt[n]{\prod_{i=1}^n D_{\Pi_{x_{i-1}}}(x_i)}. \quad (2)$$

This definition extends that of statistical depth for multivariate distributions. Indeed, when $n = 1$, we have $D_{\Pi}((x_0, x_1)) = D_{\Pi_{x_0}}(x_1)$. The rationale behind it is obvious: *the deeper in average the transitions forming the path, the deeper the trajectory*. In particular, if an impossible transition $x_{i-1} \rightarrow x_i$ is present in the trajectory \mathbf{x} (*i.e.* $D_{\Pi_{x_{i-1}}}(x_i) = 0$), its Markov depth equals 0, *i.e.* $D_{\Pi}(\mathbf{x}) = 0$. Provided that the depth functions D_{Π_x} can be easily computed (or estimated, see the analysis below), the Markovian sample path depth permits to evaluate and compare the depth of paths of any (finite) length.

Example 3. (MARKOVIAN HALF-SPACE DEPTH) If the Markov depth is based on the half-space depth introduced in [49] (see also section A1 in the Appendix), it takes the form: $\forall n \geq 1, \forall \mathbf{x} = (x_0, \dots, x_n) \in E^{n+1}$,

$$D_{\Pi}(\mathbf{x}) = \sqrt[n]{\prod_{i=1}^n \inf_{u \in \mathbb{S}_{d-1}} \Pi_{x_{i-1}}(\mathcal{H}_{u,x_i})}, \quad (3)$$

where $\mathcal{H}_{u,x} = \{y \in \mathbb{R}^d : \langle u, y - x \rangle \geq 0\}$ for all $(u, x) \in \mathbb{S}_{d-1} \times E$.

Example 4. (MARKOV IRW-DEPTH) In order to avoid optimization issues, various alternatives to Tukey's depth functions have been proposed, see *e.g.* [13]. In [42] (see also [12]), a new data depth, referred to as the Integrated Rank-Weighted (IRW) depth, is defined by using an integral over the sphere \mathbb{S}^{d-1} instead of the infimum. When based on the IRW-depth, the Markov depth is given by: $\forall n \geq 1, \forall \mathbf{x} = (x_0, \dots, x_n) \in E^{n+1}$,

$$D_{\Pi}(\mathbf{x}) = \sqrt[n]{\prod_{i=1}^n \int_{u \in \mathbb{S}_{d-1}} \Pi_{x_{i-1}}(\mathcal{H}_{u,x_i}) \omega_{d-1}(du)}, \quad (4)$$

where ω_{d-1} is the spherical probability measure on \mathbb{S}_{d-1} . The main advantage of the IRW depth is of computational nature, the integrals w.r.t. ω_{d-1} involved in (4) can be approximated by Monte Carlo procedures: $Z/\|Z\| \sim \omega_{d-1}$ as soon as $Z \sim \mathcal{N}(0, \mathcal{I}_d)$ is a standard centered Gaussian.

In addition to its interpretability, the concept introduced has a number of advantages, as it inherits many properties from the notion of multivariate statistical depth it relies on (see Theorems 1, 2 and 3). As discussed in the following, the choice of D must be weighed against the verification of the desirable properties and the availability of efficient algorithms for computation in the case of empirical distributions (*i.e.* for computing $D_{\hat{P}}$, where \hat{P} is a statistical version of the distribution P considered).

Main Properties. Before investigating the theoretical properties of the Markovian path depth and inference issues, we state the following result, revealing that the Markov depth of a positive recurrent chain \mathbf{X} , evaluated at a random path of length $n + 1$, is *stochastically stable* as $n \rightarrow \infty$, meaning that its distribution asymptotically converges to a Gaussian limit as the path length n increases.

Proposition 1. (LIMIT DISTRIBUTION) *Assume that \mathbf{X} is positive recurrent with stationary distribution μ and that $\log(D_{\Pi_x}(y))$ is integrable w.r.t. $\mu d(x)\Pi_x(dy)$ in E^2 . Then, for any initial distribution ν , we have that $D_{\Pi}(X_0, X_1, \dots, X_n)$ converges almost surely to $D_{\infty}(\Pi)$ as $n \rightarrow \infty$, where*

$$D_{\infty}(\Pi) = \exp \left(\int_{(x,y) \in E^2} \log(D_{\Pi_x}(y)) \Pi_x(dy) \mu(dx) \right). \quad (5)$$

If in addition $\log(D_{\Pi_x}(y))$ is square integrable w.r.t. $\mu d(x)\Pi_x(dy)$, then we have that, as n goes to ∞ ,

$$\sqrt{n} \left(D_{\Pi}(X_0, X_1, \dots, X_n) - D_{\infty}(\Pi) \right)$$

converges in distribution to a centered normal random variable. The exact form of the asymptotic variance is given by (A6.11) in the Supplementary Material.

Our next result shows that the Markovian sample path depth D_{Π} inherits most of its statistical properties from the multivariate depth D it is based on, and for most choices of D , it satisfies the properties given in Definition 1.

Theorem 1. *Let D be a statistical depth on E and D_{Π} be the Markovian sample path depth based on the latter. The following assertions hold true.*

- (i) *The Markovian depth D_{Π} satisfies (M0).*
- (ii) *If D satisfies (P1), then D_{Π} satisfies (M1).*
- (iii) *Assume that D fulfills the following stronger version of property (P2): $\forall M > 0, \sup_{||x|| \leq M} D_{\Pi_x}(y) \rightarrow 0$ as $||y|| \rightarrow \infty$. Then D_{Π} satisfies (M2).*

In addition to the above properties, D_{Π} also satisfies the following property, which can be viewed as a variation of (P3).

Proposition 2. (MAXIMALITY AT PATHS OF CENTERS) *Let Π be a transition probability on \mathbb{R}^d . Assume that D fulfills property (P3) for a given notion of symmetry, that the distribution $\Pi_x(dy)$ on E is 'symmetric' w.r.t. a center $\theta(x) \in E$ for any $x \in E$ and that $x \in E \mapsto D_{\Pi_x}(\theta(x))$ is constant. Then, for any initial value $x_0 \in \mathbb{R}^d$ and any $n \geq 1$, the trajectory $(x_0, \theta^{(1)}(x_0), \dots, \theta^{(n-1)}(x_0))$ is of maximal Markov depth D_{Π} , where $\theta^{(1)}(x_0) = \theta(x_0)$ and $\theta^{(i+1)}(x_0) = (\theta \circ \theta^{(i)})(x_0)$ for $i \geq 1$.*

We point out that the paths considered in Proposition 2 above are not symmetry centers for \mathbf{X} 's law in general.

Continuity (in x , in Π). The following classic technical conditions are involved in the subsequent study of the continuity properties of the Markov depth.

(P5) (CONTINUITY IN x) For any law P on \mathbb{R}^d , the mapping $x \in \mathbb{R}^d \mapsto D_P(x)$ is continuous.

- (P6) (UNIFORM WEAK CONTINUITY IN P) For any probability distributions P and P_n on \mathbb{R}^d s.t. $P_n \Rightarrow P$ as $n \rightarrow \infty$, we have $\sup_{x \in \mathbb{R}^d} |D_{P_n}(x) - D_P(x)| \rightarrow 0$ as $n \rightarrow \infty$.
- (P6') (WEAK CONTINUITY IN P) For any probability distributions P and P_n on \mathbb{R}^d s.t. $P_n \Rightarrow P$ as $n \rightarrow \infty$, we have: $\forall x \in \mathbb{R}^d$, $|D_{P_n}(x) - D_P(x)| \rightarrow 0$ as $n \rightarrow \infty$.
- (P7) (WEAK FELLER CONDITION) Denoting by $\mathcal{M}_1(E)$ the set of probability measures on E equipped with the weak convergence topology, the function $x \in E \mapsto \Pi_x$ mapping E to $\mathcal{M}_1(E)$ is continuous.

Properties (P5) and (P6) are satisfied by many notions of statistical depth (see section A1). The result below reveals that the Markov depth inherits its continuity properties from those of the multivariate depth D involved in its definition.

Theorem 2. *The following assertions hold true.*

- (i) (CONTINUITY IN \mathbf{x}) Suppose that properties (P5), (P6) and (P7) are fulfilled. Then, the mapping $\mathbf{x} \in \mathbb{T} \mapsto D_{\Pi}(\mathbf{x})$ is continuous.
- (ii) (CONTINUITY IN Π) Suppose that (P6') holds. Let Π and $\Pi^{(n)}$ be transition probabilities on E s.t. $\forall x \in E$, $\Pi_x^{(n)} \Rightarrow \Pi_x$ as $n \rightarrow \infty$. Then: $\forall \mathbf{x} \in \mathbb{T}$, $D_{\Pi^{(n)}}(\mathbf{x}) \rightarrow D_{\Pi}(\mathbf{x})$.

Sampling Versions and Estimation. The Markovian depth D_{Π} is unknown in general, just like the transition probability Π . In practice, a *plug-in* strategy based on an empirical counterpart $\hat{\Pi}$ of Π and must be implemented, using $D_{\hat{\Pi}}$ as an estimate of D_{Π} . Refer to A3 in the Supplementary Material for a description of inference techniques dedicated to the statistical estimation of Π with (non-asymptotic) guarantees. The following condition, which can be viewed as strong version of (P6), permits to link Π 's estimation error with that of D_{Π} .

- (P6'') (LIPSCHITZ CONDITION) Let \mathcal{A} be a collection of Borel subsets of \mathbb{R}^d . There exists a finite constant C_d such that, for any probability distributions P and Q on \mathbb{R}^d , we have: $\sup_{x \in \mathbb{R}^d} |D_P(x) - D_Q(x)| \leq C_d \|P - Q\|_{\mathcal{A}}$, where $\|P - Q\|_{\mathcal{A}} := \sup_{A \in \mathcal{A}} |P(A) - Q(A)|$.

Property (P6'') is fulfilled by various multivariate depths for specific classes \mathcal{A} (see Section A1 of the appendix). As shown by the theorem below, non-asymptotic guarantees for sampling versions of the Markov depth can be established under this condition.

Theorem 3. *Let $n \geq 1$ and $\mathbf{x} \in E^{n+1}$. Consider two transition probabilities Π and $\hat{\Pi}$ on E . Suppose that D fulfills (P6'') and there exists $\epsilon > 0$ s.t. $\min\{D_{\hat{\Pi}_i}(x_{i+1}), D_{\Pi_i}(x_{i+1})\} > \epsilon$ for $i < n$. We have*

$$|D_{\Pi}(\mathbf{x}) - D_{\hat{\Pi}}(\mathbf{x})| \leq \frac{7}{4} C_d \frac{D_{\Pi}(\mathbf{x})}{\epsilon} \max_{i=0, \dots, n-1} \|\Pi_{x_i} - \hat{\Pi}_{x_i}\|_{\mathcal{A}}. \quad (6)$$

The above result deserves comments. It proves that error bounds (in expectation, in probability) for point-wise deviations between $D_{\Pi}(\mathbf{x})$ and $D_{\hat{\Pi}}(\mathbf{x})$ can be straightforwardly deduced from bounds for the maximal deviations over the class \mathcal{A} between the transition probability Π_x and its estimator $\hat{\Pi}_x$ at the successive points x forming the path \mathbf{x} considered. In addition, as $\min_{1 \leq i < n} D_{\Pi_{x_{i-1}}}(x_i)$ gets smaller, the factor $D_{\Pi}(\mathbf{x})/\epsilon$ on the right hand side of (6) increases to ∞ , showing that the smaller the Markov depth value to be estimated with a given error bound, the higher the accuracy of the transition probability estimator required.

Computational issues. Various efficient algorithmic procedures have been designed to compute the values taken by a depth function in the multivariate case, based on a discrete, empirical distribution [38]. The approach below shows how to use the latter to estimate the values taken by a Markovian sample path depth.

Algorithm 1: Estimation of $D_{\hat{\Pi}}(\mathbf{x})$

Input: Path $\mathbf{x} = (x_0, \dots, x_n)$ with $n \geq 1$ in \mathbb{T} , transition probability $\hat{\Pi}$ and precision control integer $M \geq 1$.

- 1 **for** $i := 0$ **to** $n - 1$ **do**
- 2 Generate M independent samples $x_{1,i}, \dots, x_{M,i}$ from $\hat{\Pi}_{x_i}$
- 3 Compute an estimator \hat{D}_i of $D_{\hat{\Pi}_{x_i}}(x_{i+1})$ based on $y_{1,i}, \dots, y_{M,i}$

Output: $D_{\hat{\Pi}}(\mathbf{x}) = \sqrt[n]{\prod_{i=1}^n \hat{D}_i}$.

Attention should be paid to the fact that the complexity of estimating the value that $D_{\hat{\Pi}}$ takes at a path of length $n + 1$ through Algorithm 1 is of order $O(ng(M, d))$, where $O(g(M, d))$ is the numerical complexity of computing the value taken by the empirical depth function $D_{\hat{\rho}}$ based on M independent samples of P . For instance, we have $g(M, d) = M^{d-1} \log M$ in the case of the half-space depth, see *e.g.* [20]. In comparison, the complexity of calculating the value taken by the multivariate depth at (x_0, \dots, x_n) , viewed as a point of $\mathbb{R}^{(n+1)d}$, based on M paths of length $n + 1$ (viewed as M sample points in $\mathbb{R}^{(n+1)d}$) is of order $O(g(M, (n+1)d))$ (namely, $M^{(n+1)d-1} \log M$ in the case of the half-space depth). As a result, the Markov depth offers considerable computational advantages over the direct use of multivariate depth when considering “long” trajectories.

4 Application to Anomaly Detection

The proposed notion of Markov depth can be used for various tasks related to the statistical analysis of Markov paths of different lengths. For reasons of space and given the importance of this task in practice, the focus is on (unsupervised) anomaly detection in this section. Applications of the Markov depth to the clustering of Markov paths of different lengths and to the problem of testing whether two collections of Markov trajectories are drawn from the same (unknown) transition probability are described in the appendix, together with dedicated numerical experiments.

Unsupervised anomaly detection. Markov chains are used in a wide variety of fields, including systems engineering to model storage systems or teletraffic data as well as time-series analysis, and (unsupervised) anomaly detection plays a crucial role in the monitoring/management of such complex systems/phenomena. Precisely, the problem considered is as follows. The objective is to identify paths \mathbf{x} that are suspicious due to their significant difference with the majority of observed sample paths. Here, an observation $\mathbf{x} = (x_0, \dots, x_n)$ with fixed length $n \geq 1$ and initial value $x_0 \in \mathbb{R}^d$ is *abnormal* when it is not the realization of the Markov chain with transition probability Π generating the *normal* (“not abnormal”, with no reference to the Gaussian law here) trajectories, *i.e.* when it is not a realization of the probability distribution $\delta_{x_0}(dx_0)\Pi(x_0, dy_1)\Pi(y_1, dy_2) \dots \Pi(y_{n-1}, dy_n)$, Π being unknown in practice of course. Based on a set of (unlabeled, but supposedly normal in vast majority) training paths, the goal is to build an anomaly scoring rule $s : \mathbb{T} \rightarrow \mathbb{R}$ permitting to assign a level of abnormality $s(\mathbf{x})$ to any future path \mathbf{x} in \mathbb{R} : the lower the score $s(\mathbf{x})$, the more suspicious the path \mathbf{x} observed ideally. Although the learning stage involves unlabeled datasets, the availability of labels is required to assess predictive performance (possibly depending on the type of anomaly considered). The gold standard in this respect is the ROC curve, *i.e.* the parameterized curve describing the rate of normal paths with a score below t (false positive rate) compared to that of abnormal paths with a score below t (true positive rate), as the t threshold varies, or its popular scalar summary, the AUC criterion (*i.e.* the Area Under the ROC Curve).

Below, we describe the two experimental contexts for which we then present the numerical results. The latter reveal that the performance of the simple method of using an empirical version of a Markov depth as the anomaly scoring function is quite similar to that of conventional techniques (which can only be used in contrast when the training/test paths are all of the same length) when considering well-identified isolated/displacement/shape anomalies (see [24]) and significantly outperforms them when the anomaly is of a dynamic nature (*i.e.* corresponding to a more or less long-lasting change in transition dynamics), in line with its original motivation. This is confirmed by the extra experiments documented in the Appendix.

Nonlinear time-series. Consider the ARCH(1) Markov chain, defined by: $X_{n+1} = m(X_n) + \sigma(X_n)\epsilon_n$ where $m : \mathbb{R} \mapsto \mathbb{R}$ and $\sigma : \mathbb{R} \mapsto \mathbb{R}_+^*$ are unknown measurable functions and ϵ_n is a sequence of i.i.d. r.v.’s with mean 0 and variance 1 independent of X_0 . Here, we have chosen $X_0 \equiv 0.5$, $m(x) = 1/(1 + \exp(-x))$ and $\sigma(x) = \psi(x + 1.2) + 1.5\psi(x - 1.2)$ where $\psi(x)$ is $\mathcal{N}(0, 1)$ ’s density function and $\epsilon_n \sim \mathcal{N}(0, 1)$. This model, introduced in [21], is widely used in Econometrics, to model the return of financial assets [6,25,22].

Queueing system. Consider now a GI/G/1 queueing system with interarrival times T_n and service times V_n where $\{T_n\}_{n \geq 0}$ and $\{V_n\}_{n \geq 0}$ are independent i.i.d. sequences with distributions V and T respectively. Denote by X_n the waiting time of the n -th customer and assume that $X_0 = 0$, then, $X_{n+1} = \max(0, X_n +$

W_n) where $W_n = V_n - T_n$, which corresponds to Example 1. Here, V and T are exponential r.v.'s with means 0.45 and, 0.5 respectively.

Generation of anomalous paths. We examine 4 types of anomalies (isolated/shock, two dynamic and shift), generated by modifying the Markov model over a path segment. For the ARCH(1) model, the isolated anomaly is simulated by setting $m(x) = 5x$ and $\sigma(x) = |x|^{1/2}$ for two steps. The first dynamic anomaly alters $m(x) = 1/(2 + \exp(-x))$ for 60% of the path, while the second takes $\sigma(x) = 0.5\sqrt{x^2 + 1}$ over 60% of the trajectory. The shift anomaly uses $m(x) \equiv 2$ for 60% of the path length.

For the queuing system, the shock anomaly is generated by using V as an exponential distribution with a mean of 2.25 over 10% of the trajectory. The first dynamic anomaly changes the interarrival time distribution T to an exponential with a mean of 0.1 over 20% of the path, simulating a period of increased customer arrivals. The second dynamic anomaly modifies the service time distribution V to $0.55\mathcal{U}$, where \mathcal{U} is uniform on $(0, 2)$, over 30% of the path, representing a period of slightly slower service times. The shift anomaly is generated by considering deterministic interarrival times $T_n = 2^{-n}$ over 25 of steps.

Table 1: AUC for anomalies in the ARCH(1) and queuing models

Anomaly type	ARCH(1)	Queuing
Shock	0.97	0.95
Dynamic anomaly I	0.71	0.90
Dynamic anomaly II	0.87	0.73
Shift	1.00	0.93

For each model we simulated one long training path ($n = 1000$) and 4 contaminated data sets, each one containing 200 paths of random length (between 50 and 200) where 50% of those contain a specific type of anomaly. Based on the long path, a kernel estimator \hat{H} (see A3) is computed and used to infer, for each trajectory, the Markov depth D_H based on the half-space depth.

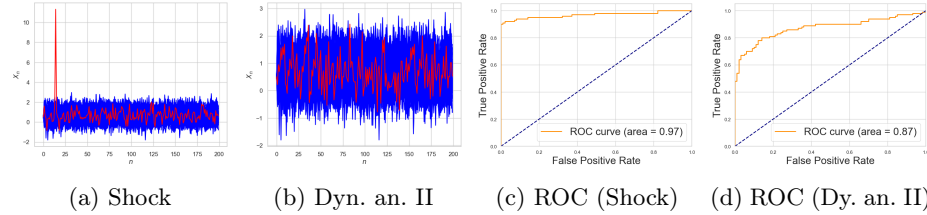


Fig. 2: Subfigures (a) and (b) illustrate anomalies in the ARCH(1) model, with normal paths shown in blue and anomalous trajectories in red. Subfigures (c) and (d) present the ROC curves of our scoring function for the shock and dynamic anomaly II scenarios.

Results and Discussion. The results in Table 1 indicate that the Markov depth detects with high accuracy classic anomalies such as shocks/shifts, see

Fig. 2a and 3b. Our approach is also capable of detecting the more challenging dynamic anomalies, see Fig. 2b and 3a. The corresponding ROC curves in Fig. 2 and 3 reveal its strong performance on the different types of anomaly considered. In Section B1, it is compared with that of alternative anomaly detection techniques, focusing on fixed-length paths since the competitors cannot straightforwardly handle variable-length paths. The results of these experiments, presented in Table 2 and Fig. 4 and 5 in the Appendix, show that our method performs similarly to the best of the competitors for classic anomalies and significantly outperforms them for dynamic ones.

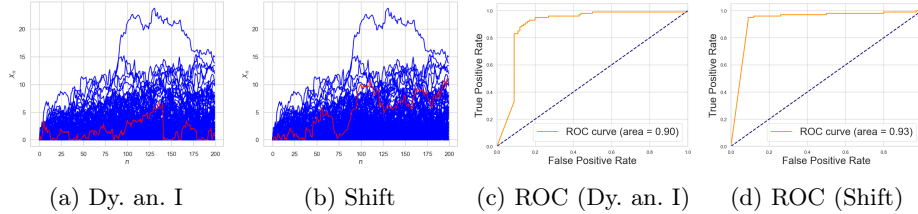


Fig. 3: Subfigures (a) and (b) show anomalies in the queuing model: blue lines are normal paths and red lines are anomalous paths. Subfigures (c) and (d) display the ROC curves of our scoring function for these types of anomalies.

5 Some Concluding Remarks and Perspectives

In this paper, we have proposed a concept of statistical depth tailored to Markov data/laws, relying on classic approaches in the multivariate setting. A list of desirable properties have been shown to be satisfied when the Markov depth is based on popular choices for the underlying multivariate depth. The concept is promoted throughout the article as a very natural way of defining an ordering on the set of trajectories of variable (finite) length, so as to extend the notions of order statistics and ranks for Markov data. Theoretical and experimental results have also been presented in this article, showing that Markov depth can be accurately estimated by its empirical version and may serve to detect anomalous paths in a reliable manner. It may be used to perform a wide variety of other statistical tasks, ranging from the design of homogeneity tests between sets of trajectories of possibly different lengths to the clustering of Markov paths through the design of dedicated visualization techniques. Beyond the experiments we have presented here for illustrative purposes only, we plan to further investigate the suitability of this tool for the analysis of Markov data.

Acknowledgments. This study was funded by a Grant of Hi! Paris foundation.

Disclosure of Interests. The authors have no competing interests to declare that are relevant to the content of this article.

References

1. Adams, T., Nobel, A.: Uniform convergence of VC classes under ergodic sampling. *Annals of Probability* **38**, 1345–1367 (2010)
2. Alquier, P., Wintenberger, O.: Model selection for weakly dependent time series forecasting. *Bernoulli* **18**, 883–913 (2012)
3. Asmussen, S.: *Applied Probability and Queues. Stochastic Modelling and FApplied Probability*, Springer New York, New York, 2nd edn. (2010)
4. Athreya, K.B., Atuncar, G.S.: Kernel estimation for real-valued markov chains. *Sankhyā: The Indian Journal of Statistics, Series A* (1961-2002) **60**(1), 1–17 (1998)
5. Basu, A.K., Sahoo, D.K.: On berry-esseen theorem for nonparametric density estimation in markov sequences. *Bulletin of Informatics and Cybernetics* (1998)
6. Bollerslev, T., Chou, R.Y., Kroner, K.F.: Arch modeling in finance: A review of the theory and empirical evidence. *Journal of Econometrics* **52** (apr 1992)
7. Bullen, P.S.: *A Dictionary of Inequalities*. CRC Press, 1 edn. (1998)
8. Burr, M.A., Fabrizio, R.J.: Uniform convergence rates for halfspace depth. *Statistics and Probability Letters* **124**, 33–40 (2017)
9. Chernozhukov, V., Galichon, A., Hallin, M., Henry, M.: Monge–kantorovich depth, quantiles, ranks and signs. *The Annals of Statistics* **45**(1), 223–256 (2017)
10. Clémenton, S.: Adaptive estimation of the transition density of a regular Markov chain by wavelet methods. *Math. Meth. Statist.* **9**(4), 323–357 (2000)
11. Clémenton, S., Ciolek, G., Bertail, P.: Statistical learning based on markovian data: Maximal deviation inequalities and learning rates. *The Annals of Mathematics and Artificial Intelligence* **88** (jan 2020)
12. Clémenton, S., Mozharovskyi, P., Staerman, G.: Affine invariant integrated rank-weighted statistical depth: properties and finite sample analysis. *Electronic Journal of Statistics* **17**(2), 3854 – 3892 (2023)
13. Cuevas, A., Fraiman, R.: On depth measures and dual statistics. a methodology for dealing with general data. *Journal of Multivariate Analysis* **100**(4), 753–766 (2009)
14. Devroye, L., Györfi, L., Lugosi, G.: *A Probabilistic Theory of Pattern Recognition*. Springer (1996)
15. Di, J., Kolaczyk, E.: Complexity-penalized estimation of minimum volume sets for dependent data. *Journal of Multivariate Analysis* **101**(9), 1910–1926 (2004)
16. Donoho, D.L., Gasko, M.: Breakdown properties of location estimates based on halfspace depth and projected outlyingness. *The Annals of Statistics* **20**, 1803–1827 (1992)
17. Dorea, C.: Strong consistency of kernel estimators for markov transition densities. *Bulletin of the Brazilian Mathematical Society* **33**, 409–418 (2002)
18. Douc, R., Moulines, E., Priouret, P., Soulier, P.: *Markov chains*. Springer Series in Operations Research and Financial Engineering, Springer (2018)
19. Dugundji, J.: *Topology*. Allyn and Bacon Series in Advanced Mathematics, Allyn and Bacon, 12th printing edn. (1978)
20. Dyckerhoff, R., Mozharovskyi, P.: Exact computation of the halfspace depth. *Computational Statistics and Data Analysis* **98**, 19–30 (2016)
21. Engle, R.F.: Autoregressive conditional heteroscedasticity with estimates of the variance of united kingdom inflation. *Econometrica* **50**(4), 987–1007 (1982)
22. Fan, J., Yao, Q.: Efficient estimation of conditional variance functions in stochastic regression. *Biometrika* **85**(3), 645–660 (1998)

23. Geenens, G., Nieto-Reyes, A., Francisci, G.: Statistical depth in abstract metric spaces. *Statistics and Computing* **33**(2), 46 (2023)
24. Hubert, M., Rousseeuw, P.J., Segaert, P.: Multivariate functional outlier detection. *Statistical Methods & Applications* **24**(2), 177–202 (2015)
25. Härdle, W., Tsybakov, A.: Local polynomial estimators of the volatility function in nonparametric autoregression. *Journal of Econometrics* **81**(1), 223–242 (1997)
26. Johnson, D., Preparata, F.: The densest hemisphere problem. *Theoretical Computer Science* **6**(1), 93–107 (1978)
27. Jörnsten, R.: Clustering and classification based on the l_1 data depth. *Journal of Multivariate Analysis* **90**(1), 67–89 (2004)
28. Karlsen, H., Tjostheim, D.: Nonparametric estimation in null recurrent time series. *The Annals of Statistics* **29** (04 2001)
29. Kuznetsov, V., Mohri, M.: Generalization Bounds for Time Series Prediction with Non-stationary Processes. In: *Proceedings of ALT'14* (2014)
30. Lacour, C.: Adaptive estimation of the transition density of a markov chain. *Annales de l'Institut Henri Poincaré (B) **43**(5)*, 571–597 (2007)
31. Lacour, C.: Nonparametric estimation of the stationary density and the transition density of a markov chain. *Stochastic Processes and their Applications* **118**(2), 232–260 (2008)
32. Liu: On a notion of data depth based upon random simplices. *The Annals of Statistics* **18**(1), 405–414 (1990)
33. Liu, R.Y., Parelis, J.M., Singh, K.: Multivariate analysis by data depth: descriptive statistics, graphics and inference, (with discussion and a rejoinder by Liu and Singh). *The Annals of Statistics* **27**(3), 783 – 858 (1999)
34. Liu, R.Y., Singh, K.: A quality index based on data depth and multivariate rank tests. *Journal of the American Statistical Association* **88** (mar 1993)
35. Liu, Z., Modarres, R.: Lens data depth and median. *Journal of Nonparametric Statistics* **23**(4), 1063–1074 (2011)
36. Meyn, S., Tweedie, R., Glynn, P.: *Markov chains and stochastic stability*. Cambridge Mathematical Library, Cambridge University Press, 2 edn. (2009)
37. Mosler, K.: Depth statistics. In: Becker, C., Fried, R., Kuhnt, S. (eds.) *Robustness and Complex Data Structures: Festschrift in Honour of Ursula Gather*, pp. 17–34. Springer (2013)
38. Mosler, K., Mozharovskyi, P.: Choosing among notions of multivariate depth statistics. *Statistical Science* **37**(3), 348–368 (2022)
39. Mozharovskyi, P.: Anomaly detection using data depth: multivariate case (2022)
40. Nagy, S., Dyckerhoff, R., Mozharovskyi, P.: Uniform convergence rates for the approximated halfspace and projection depth. *Electronic Journal of Statistics* **14**(2), 3939 – 3975 (2020)
41. Nagy, S., Gijbels, I., Omelka, M., Hlubinka, D.: Integrated depth for functional data: statistical properties and consistency. *ESAIM: PS* **20**, 95–130 (2016)
42. Ramsay, K., Durocher, S., Leblanc, A.: Integrated rank-weighted depth. *Journal of Multivariate Analysis* **173**, 51–69 (2019)
43. Rio, E.: *Asymptotic Theory of Weakly Dependent Random Processes* (2017)
44. Sart, M.: Estimation of the transition density of a markov chain. *Annales de l'Institut Henri Poincaré (B) Probability and Statistics* **50**(3), 1028–1068 (2014)
45. Shi, X., Zhang, Y., Fu, Y.: Two-sample tests based on data depth. *Entropy* **25**(2) (2023)
46. Staerman, G., Mozharovskyi, P., Clémenccon, S.: The area of the convex hull of sampled curves: a robust functional statistical depth measure. In: *International Conference on Artificial Intelligence and Statistics*. pp. 570–579. PMLR (2020)

47. Steinwart, I., Christmann, A.: Fast learning from non-i.i.d. observations. *NIPS* pp. 1768–1776 (2009)
48. Steinwart, I., Hush, D., Scovel, C.: Learning from dependent observations. *Journal of Multivariate Analysis* **100**(1), 175–194 (2009)
49. Tukey, J.W.: Mathematics and the picturing of data. In: *Proceedings of the International Congress of Mathematicians, Vancouver, 1975.* vol. 2, pp. 523–531. Canadian Mathematical Congress (1975)
50. van der Vaart, A.: *Asymptotic Statistics*. Cambridge University Press (1998)
51. Zuo, Y., Serfling, R.: General notions of statistical depth function. *The Annals of Statistics* **28**(2), 461–482 (2000)

Appendix

The Appendix is organized in two parts: Part A provides mathematical background, examples, and detailed technical proofs of the results presented in the main article. Part B offers expanded descriptions of the experiments from Section 4 along with additional numerical examples.

A Technical appendix

A1 Statistical Depths of Multivariate Distributions

Here we describe some well known multivariate statistical depth functions and we state the validity of the properties (P1)-(P6') described in section 2.1

Halfspace depth. The halfspace depth (HD), introduced by [49], is the first and most widely known example of a multivariate depth function. For a point $x \in E$ and a probability distribution $P \in \mathcal{P}(\mathcal{B}(E))$, $D_P(x)$ is defined as infimum of the measures, according to P , of the halfspaces containing x , that is $HD_P(x) = \inf_{u \in \mathbb{S}_{d-1}} \{P(\mathcal{H}_{u,x})\}$, where $\mathcal{H}_{u,x} = \{y \in \mathbb{R}^d : \langle u, y - x \rangle \geq 0\}$. The validity of the properties (P1) to (P4) for all $P \in \mathcal{P}(\mathcal{B}(E))$ was proved in Theorem 2.1 of [51], while the property (P5) was established in Lemma 6.1 in [16]. Regarding (P6), Theorem A.3 of [41] shows that it holds for all probability measures, P such that $P(L) = 0$ for all hyperplanes $L \subset E$. Property (P6'') trivially holds for $\mathcal{A} = \{H : H \text{ open half-spaces of } \mathbb{R}^d\}$. Several algorithms have been proposed for the exact computation of HD , with a computational complexity of $O(n^{d-1} \ln n)$ (see [20,40] for an analysis on this subject) and it has been established that determining the exact HD of a single point in arbitrary dimensions, based on a sample of n points, is NP-hard [26].

Lens depth. Let x_1 and x_2 be two points in E and $\|\cdot\|$ be a norm in E . The lens $L(x_1, x_2)$ of x_1 and x_2 is defined as the intersection of the closed balls with radius $\|x_1 - x_2\|$, and centered at x_1 and x_2 . Using this concept, [35] defined the *lens depth* (LD) of a point $x \in E$ and a probability $P \in \mathcal{P}(\mathcal{B}(E))$ as the probability that x belongs to the random lens $L(X_1, X_2)$, where X_1 and X_2 are two independent random vectors sampled from P . LD is orthogonally invariant when using the Euclidean distance on and it satisfies (P2) (see [35]). Examples 1, 2 and 3 in [23] show that properties (P3) and (P4) are not satisfied in general. Sections 3.3 and 3.4 in [23] established the validity of (P5) and (P6') under weak conditions. The computational efficiency of its sampled version is $O(n^2)$ [38].

Mahalanobis depth. Given a d -dimensional distribution P with expectation μ_P and covariance matrix Σ_P , the Mahalanobis norm of $x \in \mathbb{R}^d$ w.r.t. P is defined as $\|x\|_{\Sigma_P}^2 = x^T \Sigma_P^{-1} x$. This norm measures the distance between the point x and the distribution P . The Mahalanobis depth is then defined as: $MD_P(x) = (1 + \|x - \mu_P\|_{\Sigma_P}^2)^{-1}$. It satisfies properties (P1) through (P5) for general distributions, and it satisfies (P6) for distributions with regular covariance matrix. Regarding the computation of its sampling version, the execution

times are virtually independent of (moderate values of) n and d (the actual complexity being $O(n)$). See [38] for more details.

A2 The Space \mathbb{T} of Finite Length Paths

In order to facilitate the exposure, we will concentrate on the case $d = 1$. The properties in the case $d > 1$ follow directly from the natural isomorphism between $(\mathbb{R}^d)^n$ and \mathbb{R}^{dn} . Denote by \mathbb{R}^∞ the *space of finite sequences over \mathbb{R}* , that is

$$\mathbb{R}^\infty = \{(x_1, x_2, \dots) \in \mathbb{R}^\mathbb{N} : \text{all but finitely many } x_i \text{ equal } 0\},$$

For every $n \in \mathbb{N}$, let $\text{In}_{\mathbb{R}^n} : \mathbb{R}^n \rightarrow \mathbb{R}^\infty$ denote the canonical inclusion $\text{In}_{\mathbb{R}^n}(x_1, \dots, x_n) = (x_1, \dots, x_n, 0, 0, \dots)$. Therefore, $\mathbb{R}^\infty = \cup_{n=1}^\infty \text{In}_{\mathbb{R}^n}(\mathbb{R}^n)$. This allows us to identify each $\text{In}_{\mathbb{R}^n}(\mathbb{R}^n)$ with its corresponding \mathbb{R}^n and \mathbb{T} with \mathbb{R}^∞ . Endow each \mathbb{R}^n with its natural Borealian topology $\mathcal{B}(\mathbb{R}^n)$. The finite topology \mathcal{T} , also called the *weak topology induced by $\{\mathcal{B}(\mathbb{R}^n)\}_{n \in \mathbb{N}}$* [19, pp. 131], is defined as follows :

$$\mathcal{T} = \{U \subset \mathbb{T} : U \cap \mathbb{R}^n \in \mathcal{B}(\mathbb{R}^n) \ \forall n \in \mathbb{N}\}.$$

The following proposition resumes the main topological properties of the space $(\mathbb{T}, \mathcal{T})$. These results can be found in sections VI.8 and A.4 in [19].

Proposition 3. (PROPERTIES OF \mathcal{T}) *The following properties hold true for \mathcal{T} .*

- (i) *The space $(\mathbb{T}, \mathcal{T})$ is complete.*
- (ii) *Each \mathbb{R}^n , as a subspace of $(\mathbb{T}, \mathcal{T})$, retains its original topology $\mathcal{B}(\mathbb{R}^n)$.*
- (iii) *If (Y, \mathcal{Y}) is a topological space, then, a function $f : \mathbb{T} \rightarrow Y$ is continuous if and only if, for all $n \in \mathbb{N}$, the restriction $f \circ \text{In}_{\mathbb{R}^n}$ is continuous as a function of $(\mathbb{R}^n, \mathcal{B}(\mathbb{R}^n))$ to (Y, \mathcal{Y}) .*
- (iv) *If $\{x_m\}_{m \in \mathbb{N}}$ converges to $x = (x_1, \dots, x_n)$ in $(\mathbb{T}, \mathcal{T})$, then there exists M such that $x_m \in \mathbb{R}^n$ for all $m \geq M$ and $x_m \rightarrow x$ in $\mathbb{R}^n, \mathcal{B}(\mathbb{R}^n)$.*
- (v) *\mathcal{T} is smallest topology that makes all the inclusions $\text{In}_{\mathbb{R}^n}$ continuous (i.e. $(\mathbb{T}, \mathcal{T})$ is a coherent space).*

A direct consequence of part (iii) of Proposition 3 is that a set $K \subset \mathbb{T}$ is compact if and only if, for all $n \in \mathbb{N}$, $K \cap \mathbb{R}^n$ is compact in $\mathcal{B}(\mathbb{R}^n)$. We will say that a sequence $\{\mathbf{x}_n\}_{n \in \mathbb{N}}$ of elements of \mathbb{T} *goes to infinity* when there exist $m, M \in \mathbb{N}$ such that $\mathbf{x}_n \in \mathbb{R}^m$ for all $n \geq M$ and the sequence $\{\mathbf{x}_n\}_{n \geq M}$ goes to infinity in $\mathcal{B}(\mathbb{R}^m)$ (i.e. $\{\|\mathbf{x}_n\|\}_{n \geq M}$ goes to infinity with n .)

A3 On Markov Kernel Inference

A kernel Π admits a density w.r.t. the measure λ if there is a non-negative function π defined in $E \times E$ such that for all $x \in E$ and $A \in \mathcal{B}(E)$ we have

$\Pi(x, A) = \int_A \pi(x, y) d\lambda(y)$. For kernels that admit a density, the most widely used estimator of π is the *Nadaraya-Watson* estimator, defined as

$$\pi_n(x, y) = \frac{\sum_{i=0}^{n-1} h_n^{-1} K(h_n^{-1}(x - X_i)) K(h_n^{-1}(y - X_{i+1}))}{\sum_{j=0}^{n-1} K(h_n^{-1}(x - X_j))}, \quad (\text{A3.7})$$

where $h_n > 0$ is a bandwidth parameter and $K : E \rightarrow \mathbb{R}$ is a bounded measurable function that satisfies $\int_E |K(x)| dx = 1$ and $\|x\| |K(x)| \rightarrow 0$ as $\|x\| \rightarrow \infty$. Consistency and asymptotic normality of this estimator was shown in [4] while strong consistency was established in [17], and Berry-Essen type inequalities were obtained in [5]. In addition to the Nadaraya-Watson estimator, various other estimators have been suggested in the literature, see for instance, [10,30,31] and the compendium [44].

Estimating the conditional cdf. When $E \subset \mathbb{R}$, for x fixed, integrating over y in equation (A3.7), and letting $G(t) := \int_{-\infty}^t K(t) dt$ we get the following consistent estimator $\hat{F}_x(y)$ of the cumulative distribution function of $X_1 | X_0 = x$

$$\hat{F}_x(y) = \frac{\sum_{i=0}^{n-1} K(h_n^{-1}(x - X_i)) G(h_n^{-1}(y - X_{i+1}))}{\sum_{j=0}^{n-1} K(h_n^{-1}(x - X_j))}, \quad (\text{A3.8})$$

therefore, the distribution function \hat{F}_x can be written as a weighted sum of the distribution functions $G(h_n^{-1}(y - X_{i+1}))$

A4 On the Symmetry Property

We now discuss the property of maximality at path of centers of the Markovian depth, showing an example of where it holds. We also discuss the concept of symmetry centers and provide an example that shows why a property like (P3) is not useful in the Markovian scenario.

Maximality at path of centers. Consider the case where $d = 1$ and the Markovian depth function $D_\Pi(\mathbf{x})$ is based on Tukey's half-space depth. In this situation, we have: $\forall (x, y) \in \mathbb{R}^2$ (c.f. [13, pp. 754])

$$D_{\Pi_x}(y) = \min \{ \Pi_x((-\infty, y]), 1 - \Pi_x((-\infty, y)) + \Pi_x(\{y\}) \}. \quad (\text{A4.9})$$

Assume that for all $x \in \mathbb{R}$, the distribution Π_x is continuous and non-degenerate. Then for all $x \in \mathbb{R}$, there is a unique $\theta(x) \in \mathbb{R}$ s.t. $\Pi_x((-\infty, \theta(x)]) = 1/2$. The point $\theta(x)$ has maximal Tukey's depth of $1/2$ with respect to the distribution Π_x . As a result, the Markov depth attains its maximum value of $1/2$ at the path $(x_0, \theta(x_0), \dots, \theta^{(n-1)}(x_0))$ for any $n \geq 1$ and $x_0 \in \mathbb{R}$. The following example shows that this situation is quite common.

Example 5. (MARKOV CHAIN WITH CONTINUOUS MARGINALS) Suppose that Π admits a non-constant density function $f(x, t)$ w.r.t. the Riemann's integral. Then, the distribution functions of Π_x are all continuous and non-degenerated, therefore their Markovian depth is maximal at path $(x_0, \theta(x_0), \dots, \theta^{(n-1)}(x_0))$ for any $n \geq 1$ and $x_0 \in \mathbb{R}$.

Many well-known Markov models have densities, for example Random Walks, Autoregressive processes and Random coefficient autoregressive models. For more examples and a detailed description, see [18, Chapter 2].

Symmetry. A way to define symmetry w.r.t. the null path $\mathbf{0}$ (*i.e.* the infinite path with all components equal to 0) in the path space is by requiring that for all $n \in \mathbb{N}$ and any Borel set $A \subset \mathbb{R}^{n+1}$: $\mathbb{P}\{(X_0, \dots, X_n) \in A\} = \mathbb{P}\{(X_0, \dots, X_n) \in -A\}$, where $-A = \{\mathbf{x} = (x_0, \dots, x_n) \in \mathbb{R}^{n+1} \text{ s.t. } (-x_0, \dots, -x_n) \in A\}$. The following example exhibits a chain that fulfills this symmetry definition, but for which the null trajectory is unrealizable.

Example 6. (UNREALIZABLE SYMMETRIC PATH) Consider the Random Walk defined as $X_0 = 0$, $X_{n+1} = X_n + \epsilon_n$ for $n \geq 0$ with $\{\epsilon_n\}_{n \geq 0}$ being an i.i.d. sequence of random variables such that $\mathbb{P}(\epsilon_n = 1) = \mathbb{P}(\epsilon_n = -1) = 1/2$. This model is symmetric w.r.t the infinite null trajectory $\mathbf{0}$, however, this trajectory is unrealizable, as $\mathbb{P}(X_{n+1} = X_n) = 0$ for all $n \in \mathbb{N}$.

A5 Examples of Markov Depths

In this section we show the form of the Markovian depth in some scenarios.

Example 7. (MARKOV TUKEY'S DEPTH) Suppose \mathbf{X} is a Markov chain with kernel Π taking values in $E \subseteq \mathbb{R}$. Let $\mathbf{x} = (x_0, \dots, x_n) \in \mathbb{T}$ be such that Π_{x_i} is a continuous random variable for $i = 0, \dots, n-1$. Then, the Markov depth D_Π^H , based on the halfspace depth has the form

$$D_\Pi^H(\mathbf{x}) = \sqrt[n]{\prod_{i=1}^n \min \{\Pi_{x_{i-1}}((-\infty, x_i]), 1 - \Pi_{x_{i-1}}((-\infty, x_i])\}}. \quad (\text{A5.10})$$

We now give the form of the sampling versions of the Markovian depth for real valued Markov chains with densities. We use the notation from section A3.

Example 8. (SAMPLING VERSIONS IN \mathbb{R}) Let \mathbf{X} be a real valued, positive recurrent Markov chain with kernel Π , having continuous density π . Suppose we have a realization $X = (X_0, \dots, X_n)$ of \mathbf{X} , and let $\mathbf{x} = (x_0, \dots, x_m) \in \mathbb{T}$. Under this hypothesis, the Nadaraya-Watson estimator (A3.8), based on X can be used, and the estimators $\hat{F}_{x_{i-1}}(y)$ of the marginal CDFs are continuous functions of y . By example 7, the sampling version of the Markov depth D_Π^H adopts the form:

$$D_{\hat{\Pi}}^H(\mathbf{x}) = \sqrt[m]{\prod_{i=1}^m \min \{\hat{F}_{x_{i-1}}(x_i), 1 - \hat{F}_{x_{i-1}}(x_i)\}},$$

where the $\hat{F}_{x_{i-1}}(x_i)$ are defined as in (A3.8). Notice that the lengths of X and \mathbf{x} do not necessarily coincide.

A6 Technical Proofs

The proofs of the theoretical results stated in the paper are detailed below.

Proof of Proposition 1: As we \mathbb{P}_ν almost-surely have: $\forall n \geq 1$,

$$D_\Pi(X_0, \dots, X_n) = \exp\left(\frac{1}{n} \sum_{i=1}^n \log(D_{\Pi_{X_{i-1}}}(X_i))\right),$$

the result straightforwardly follows from the SLLN and the CLT for additive functionals of aperiodic Harris recurrent Markov chains (refer to *e.g.* Theorem 4.1 in [28]), combined with the delta method applied to the differentiable function $x \mapsto \exp(x)$ (see *e.g.* Theorem 3.1 in [50]). The asymptotic variance is given by

$$\sigma_\Pi^2 = \int_{(x,y)} \log^2(D_{\Pi_x}(y)) \mu(dx) \Pi_x(dy) - \int_x \left(\int_y \log(D_{\Pi_x}(y)) \Pi(x, dy) \right)^2 \mu(dx). \quad (\text{A6.11})$$

Proof of Theorem 1: *Independence from the initial law:* This property follows directly from definition 2 as the Markovian sample path depth is defined in terms of the transition probability kernel only.

Affine invariance: Let $f(x) = Ax + b$ be an affine invariant transformation. From the definition 2, it is clear that if we show $D_{f(\Pi)_{f(y_0)}}(f(y_1)) = D_{\Pi_{y_0}}(y_1)$ for all, $y_0, y_1 \in E$ then the claim of the theorem follows immediately.

Denote by F_{y_0} the distribution of $f(Y)$, where Y is a random variable with distribution Π_{y_0} . The affine invariance of D implies that

$$D_{F_{y_0}}(f(y_1)) = D_{\Pi_{y_0}}(y_1). \quad (\text{A6.12})$$

On the other hand, notice that, for any $C \in \mathcal{B}(E)$ and $y \in E$ we have

$$f(\Pi)(y, C) = \mathbb{P}(f(X_1) \in C | f(X_0) = y) = \Pi(f^{-1}(y), f^{-1}(C)),$$

therefore, $f(\Pi)_{f(y_0)}(C) = \Pi_{y_0}(f^{-1}(C)) = \Pi_{y_0}(f^{-1}(C)) = F_{y_0}(C)$, which shows that the distributions F_{y_0} and $f(\Pi)_{f(y_0)}$ coincide. The result now follows from (A6.12).

Vanishing at infinity: We need the following lemma.

Lemma 1. *Let $\mathbf{x} = (x_0, \dots, x_m) \in E^{m+1}$. For any $\epsilon > 0$, if there is j such that $D(x_j, \Pi_{x_{j-1}}) < \epsilon$, then $D_\Pi(\mathbf{x}) < \epsilon^{1/m}$.*

Proof (Lemma 1). Using that $0 < D < 1$, we have $\sqrt[m]{\prod_{i=1}^m D_{\Pi_{x_{i-1}}}(x_i)} \leq \epsilon^{1/m}$.

Let $\{\mathbf{x}_n\}_{n=1}^\infty \subset \mathbb{T}$ be a sequence that tends to infinity in \mathcal{T} . The topology of the torus implies that there exists an integer m such $\mathbf{x}_n \in E^{m+1}$ for n big enough and that $\|\mathbf{x}_n\|_\infty := \max_{0 \leq i \leq m} \|x_{i,n}\|$ tends to infinity with n . Suppose that $D_\Pi(x_n)$ does not converge to 0, then, there is an $\epsilon > 0$ such that $D_\Pi(x_n) > \epsilon$ for

all n . Therefore, by the contrapositive of Lemma 1, for all $n \in \mathbb{N}$ and $i = 0, \dots, m$ we have $D_{\Pi_{x_{i-1,n}}}(x_{i,n}) > \epsilon^m$.

Because $D_{\Pi_{x_0}}$ satisfies (P2), we have that there exists C_1 such that $D_{\Pi_{x_0}}(y) < \epsilon^m$ for all y with $\|y\| > C_1$, therefore, $\|x_{1,n}\| \leq C_1$ for all n . By the same reasoning, but using that $\sup_{\|x\| \leq C_1} D_{\Pi_x}(y) \rightarrow 0$ as $\|y\| \rightarrow \infty$, we obtain that there exists C_2 such that $\|x_{2,n}\| \leq C_2$ for all n . Repeating the same argument for $i = 2, \dots, m$, we get that the sequences $\{x_{2,n}\}_{n \geq 1}, \dots, \{x_{m,n}\}_{n \geq 1}$ are all bounded, therefore $\|\mathbf{x}_n\|_\infty$ is also bounded, which contradicts our assumption that $\|\mathbf{x}_n\|_\infty$ tends to infinity.

Proof of Proposition 2: This is a direct consequence of the monotonicity of the exponential and logarithmic functions.

Proof of Theorem 2: *Continuity in \mathbf{x} :* If \mathbf{x}_n is a sequence in \mathbb{T} that converges to \mathbf{x} , then $\mathbf{x}_n \in E^{m+1}$ for n big enough. Moreover, $\mathbf{x}_n = (x_{0,n}, \dots, x_{m,n})$ converges to $\mathbf{x} = (x_0, \dots, x_m)$ in E^{m+1} if and only if $x_{i,n} \rightarrow x_i$ in E for $i = 1, \dots, m$. Notice that for each $i = 1, \dots, m$ and n big enough we have

$$\begin{aligned} |D_{\Pi_{x_{i-1,n}}}(x_{i,n}) - D_{\Pi_{x_{i-1}}}(x_i)| &\leq |D_{\Pi_{x_{i-1,n}}}(x_{i,n}) - D_{\Pi_{x_{i-1}}}(x_{i,n})| + \\ &\quad |D_{\Pi_{x_{i-1}}}(x_{i,n}) - D_{\Pi_{x_{i-1}}}(x_i)|. \end{aligned}$$

The first term on the right hand side of the previous inequality tends to 0 as n tends to infinity thanks to property (P6) of D and the weakly convergence of $\Pi_{x_{i-1,n}}$ to $\Pi_{x_{i-1}}$. Similarly, the second term goes to 0 as n goes to infinity in virtue of (P5). This shows that $D_{\Pi_{x_{i-1,n}}}(x_{i,n}) \rightarrow_n D_{\Pi_{x_{i-1}}}(x_i)$ for $i = 1, \dots, m$. The continuity of D_{Π} now follows from (2) and the continuity of $y \mapsto \sqrt[m]{y}$.

Continuity in Π : For each $\mathbf{x} \in \mathbb{T}$ we have that $|D_{\Pi^{(n)}}(\mathbf{x}) - D_{\Pi}(\mathbf{x})|$ is smaller than $\max_{0 \leq i \leq m-1} |D_{\Pi_{x_i}^{(n)}}(x_{i+1}) - D_{\Pi_{x_i}}(x_{i+1})|$, the result now follows from (P6').

Proof of Theorem 3: We prove the following stronger version of Theorem 3

Theorem 4. *Let $n \geq 1$ and $\mathbf{x} = (x_0, \dots, x_n) \in E^{n+1}$. Consider two transition probabilities Π and $\hat{\Pi}$ on E . Suppose that D fulfills property (P6'') and $C_d \|\Pi_{x_i} - \hat{\Pi}_{x_i}\|_{\mathcal{A}} < \min\{D_{\Pi_{x_i}}(x_{i+1}), D_{\hat{\Pi}_{x_i}}(x_{i+1})\}$ for $i = 1, \dots, n$. Then,*

$$|D_{\Pi}(\mathbf{x}) - D_{\hat{\Pi}}(\mathbf{x})| \leq \frac{7}{4} C_d \frac{D_{\Pi}(\mathbf{x})}{H_{\Pi, \hat{\Pi}}(\mathbf{x})} \max_{i=0, \dots, n-1} \|\Pi_{x_i} - \hat{\Pi}_{x_i}\|_{\mathcal{A}}, \quad (\text{A6.13})$$

where

$$H_{\Pi, \hat{\Pi}}(\mathbf{x}) := \frac{n}{\sum_{i=0}^{n-1} 1/\sqrt{D_{\Pi_{x_i}}(x_{i+1}) D_{\hat{\Pi}_{x_i}}(x_{i+1})}}$$

represents the harmonic mean of $\sqrt{D_{\Pi_{x_i}}(x_{i+1}) D_{\hat{\Pi}_{x_i}}(x_{i+1})}$, $i = 0, \dots, n-1$.

Proof (Theorem 4). Let $h_i = D_{\hat{\Pi}_{x_i}}(x_{i+1}) - D_{\Pi_{x_i}}(x_{i+1})$, then, we can write $\ln D_{\hat{\Pi}_{x_i}}(x_{i+1}) = \ln D_{\Pi_{x_i}}(x_{i+1}) + \ln(1 + h_i/D_{\Pi_{x_i}}(x_{i+1}))$ and

$$|D_{\Pi}(\mathbf{x}) - D_{\hat{\Pi}}(\mathbf{x})| = D_{\Pi}(\mathbf{x}) \left| 1 - \exp \left(\frac{1}{n} \sum_{i=0}^{n-1} \ln \left(1 + \frac{h_i}{D_{\Pi_{x_i}}(x_{i+1})} \right) \right) \right|. \quad (\text{A6.14})$$

By (P6'') and our hypothesis, we have

$$|h_i| \leq C_d \|\Pi_{x_i} - \hat{\Pi}_{x_i}\|_{\mathcal{A}} < \min\{D_{\Pi_{x_i}}(x_{i+1+}), D_{\hat{\Pi}_{x_i}}(x_{i+1})\}$$

for $i = 0, \dots, n-1$, therefore, $|h_i| / \min\{D_{\Pi_{x_i}}(x_{i+1}), D_{\hat{\Pi}_{x_i}}(x_{i+1})\} < 1$ for all i . Using the inequality $|\ln(1+t)| \leq |t|/\sqrt{1+t}$, valid for $t \geq -1$ [7, pp. 160], and that $(h_i/D_{\Pi_{x_i}}(x_{i+1}))(1+h_i/D_{\Pi_{x_i}}(x_{i+1}))^{-1} = h_i/D_{\hat{\Pi}_{x_i}}(x_{i+1})$, we get

$$\left| \ln \left(1 + \frac{h_i}{D_{\Pi_{x_i}}(x_{i+1})} \right) \right| \leq \frac{|h_i|}{\sqrt{D_{\Pi_{x_i}}(x_{i+1}) D_{\hat{\Pi}_{x_i}}(x_{i+1})}}, \quad i = 0, \dots, n-1 \quad (\text{A6.15})$$

which is smaller than 1. Therefore, $|\frac{1}{n} \sum_{i=0}^{n-1} \ln(1 + h_i/D_{\Pi_{x_i}}(x_{i+1}))| < 1$. This allows us to apply the inequality $|1 - e^t| < \frac{7}{4}|t|$ (valid for $|t| < 1$) [7, pp. 82] on equation (A6.14), which combined with equation (A6.15) shows that

$$|D_{\Pi}(\mathbf{x}) - D_{\hat{\Pi}}(\mathbf{x})| \leq \frac{7}{4} D_{\Pi}(\mathbf{x}) \frac{1}{n} \sum_{i=0}^{n-1} \frac{|h_i|}{\sqrt{D_{\Pi_{x_i}}(x_{i+1}) D_{\hat{\Pi}_{x_i}}(x_{i+1})}}.$$

Equation (A6.13) now follows from (P6'').

Now we proceed to the proof of Theorem 3. Notice that if $C_d \|\Pi_{x_i} - \hat{\Pi}_{x_i}\|_{\mathcal{A}}$ is greater than $\min\{D_{\Pi_{x_i}}(x_{i+1}), D_{\hat{\Pi}_{x_i}}(x_{i+1})\}$ for some $i \in \{0, \dots, n-1\}$, then $C_d \max_{i=0, \dots, n-1} \|\Pi_{x_i} - \hat{\Pi}_{x_i}\|_{\mathcal{A}} > \epsilon$, which implies that the right hand side of (6) is bigger than $(7/4)D_{\Pi}(\mathbf{x})$. In this case, the inequality is trivially satisfied because $D_{\Pi}(\mathbf{x})$ and $D_{\hat{\Pi}}(\mathbf{x})$ are both between 0 and 1. On the other hand, when $C_d \|\Pi_{x_i} - \hat{\Pi}_{x_i}\|_{\mathcal{A}}$ is smaller than $\min\{D_{\Pi_{x_i}}(x_{i+1}), D_{\hat{\Pi}_{x_i}}(x_{i+1})\}$ for all i , we can apply Theorem 4. Equation (6) now follows from (A6.13) using that $\sqrt{D_{\Pi_{x_i}}(x_{i+1}) D_{\hat{\Pi}_{x_i}}(x_{i+1})}$ is greater than $\min\{D_{\hat{\Pi}_i}(x_{i+1}), D_{\Pi_i}(x_{i+1})\} > \epsilon$.

B Additional Numerical Experiments

This appendix provides additional numerical experiments demonstrating the practical utility of the Markov depth concept. Section B1 continues the experiments from Section 4 by comparing our method with competitors. Section B2 presents Markovian DD-plots for clustering, and Section B3 shows how to use Markov depth for homogeneity testing. The code for all experiments, as well as high resolution versions of the images presented, is available at https://github.com/statsmarkov/depth_markov.

B1 Anomaly Detection: a Benchmark Study

In order to compare our proposal (D_{Π}) against the most commonly used methods for anomaly detection in multivariate data, specifically Isolation Forest (IF),

Local Outlier Factor (LOF), and Mahalanobis Depth (MD), we must limit our analysis to scenarios where all trajectories are of equal length. For this experiment, we generated 8 datasets (one for each type of anomaly and model), each containing 100 trajectories of 200 points, with 5% of the trajectories exhibiting a specific type of anomaly. We then applied our method alongside the previously mentioned anomaly detection algorithms to each dataset. For IF and LOF we have used the implementation contained in the python library *sklearn*, while for the Mahalanobis depth we have used the Python package *data-depth*, all parameters used in the algorithms were set to their default values. For our Markovian depth algorithm, we generated a sample of 10 trajectories of size 200 in order to obtain an estimator of the kernel. The ROC curves (Fig. 4 and 5) and the AUC (Table 2) clearly show that, for classical anomalies (shock and shift) our method performs similarly to the best between IF, LOF and MD, while for dynamic anomalies, it outperforms it.

Table 2: Comparison of the AUC for different classifiers.

Anomaly type	ARCH(1) model				Queuing model			
	IF	LOF	MD	D_{II}	IF	LOF	MD	D_{II}
Shock	0.75	0.82	0.68	0.85	0.67	0.98	0.44	0.98
Dynamic anomaly I	0.42	0.63	0.52	0.84	0.59	0.80	0.80	0.94
Dynamic anomaly II	0.68	0.90	0.91	0.99	0.64	0.55	0.50	0.85
Shift	1	1	0.6	1	0.93	0.99	0.69	0.98

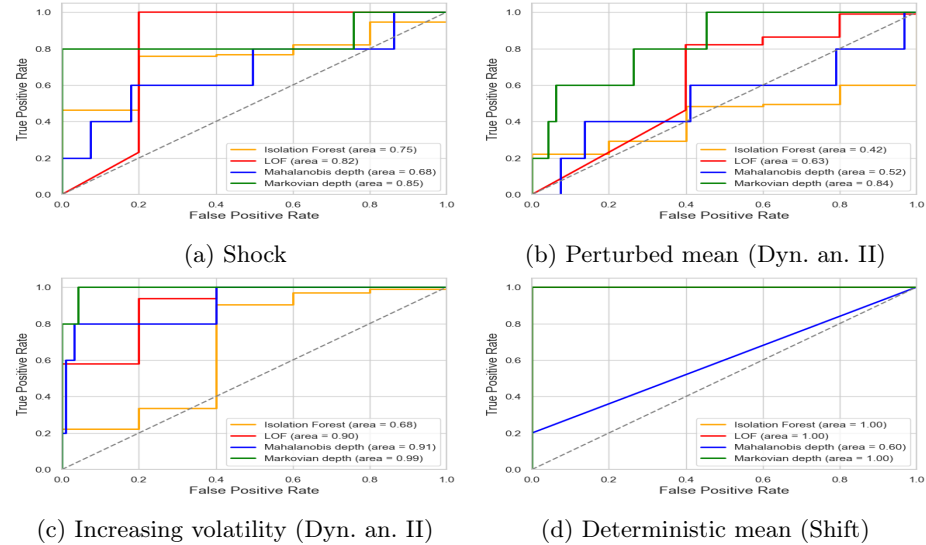


Fig. 4: ROC curves for each type of anomaly in the ARCH(1) model.

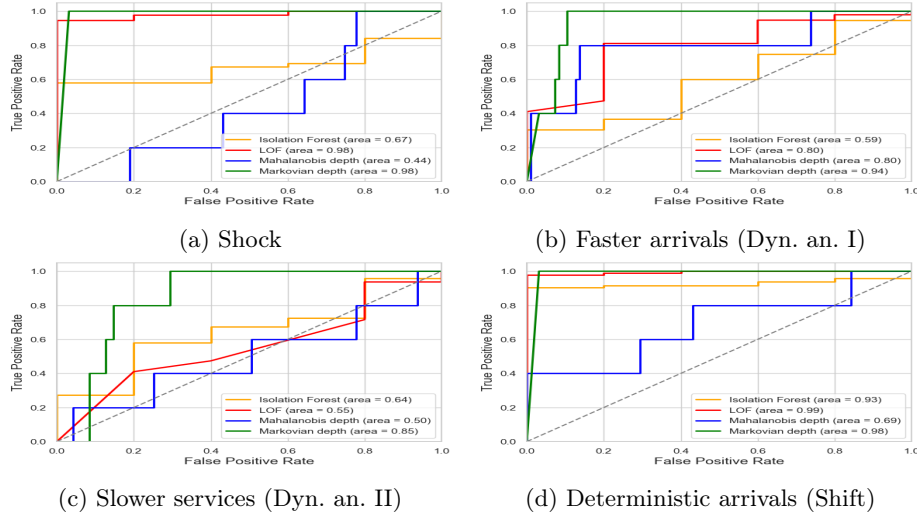


Fig. 5: ROC curves for each type of anomaly in the queuing model.

B2 Clustering Markov Paths

The infinite dimension of Markov chains makes it challenging to visualize the data and understand the underlying structure. As it was shown in Figure 1a even in the case $d = 1$ and constant path length, plotting the paths as a function of n is not very useful, as the trajectories tend to occupy a vast part of the space due to the ergodicity. Markovian depth functions can be effectively utilized to develop a visual diagnostic tool for Markovian paths, building upon the Depth vs. Depth plot (DD-plot), first introduced in [33] for multivariate data. For two sets of Markov trajectories $\mathcal{X} = \{\mathbf{x}_1, \dots, \mathbf{x}_{n_1}\}$ and $\mathcal{Y} = \{\mathbf{y}_1, \dots, \mathbf{y}_{n_2}\}$ with corresponding kernel estimators $\hat{\Phi}$ and $\hat{\Psi}$, the Markovian DD-plot is obtained by plotting in the Euclidean plane the points $\{(D_{\hat{\Phi}}(\mathbf{x}), D_{\hat{\Psi}}(\mathbf{x})) : \mathbf{x} \in \mathcal{X} \cup \mathcal{Y}\}$.

To illustrate the use of DD-plots, we have generated 5 data sets, each one containing 50 trajectories of random lengths (between 50 and 200 steps). These datasets, labeled $\mathcal{X}, \mathcal{Y}_a, \mathcal{Y}_b, \mathcal{Y}_c, \mathcal{Y}_d$, are constructed following an ARCH(1) model with the parameters stated in Table 3. Figure 6, shows the DD-plots of \mathcal{X} (blue points) and \mathcal{Y}_i (yellow stars) for $i = a, b, c, d$. It can be readily seen that, the more “similar” the distributions of both sets are (in the sense of the parameters used to generate the data), the more commingled the points in the DD-plot are. Notice that the samples in \mathcal{Y}_a have the same distribution as the samples in \mathcal{X} , then, it is expected that the DD-plot shows a straight line, see 6a. Conversely, the more the distributions diverge, the more separated the points (see Fig. 6d).

B3 Homogeneity Testing

The proposed Markovian depth can further be used to provide a formal inference, which we exemplify as a nonparametric test of homogeneity between

Table 3: Parameters of the ARCH(1) model used in Figure 6

Dataset	$m(x)$	$\sigma(x)$
\mathcal{X}	$(1 + \exp(-x))^{-1} \psi(x + 1.2) + 1.5\psi(x - 1.2)$	
\mathcal{Y}_a	$(1 + \exp(-x))^{-1} \psi(x + 1.2) + 1.5\psi(x - 1.2)$	
\mathcal{Y}_b	$(2 + \exp(-x))^{-1} \psi(x + 1.2) + 1.5\psi(x - 1.2)$	
\mathcal{Y}_c	$(4 + \exp(-x))^{-1} \psi(x + 1.2) + 1.5\psi(x - 1.2)$	
\mathcal{Y}_d	$(1 + \exp(-x))^{-1}$	1

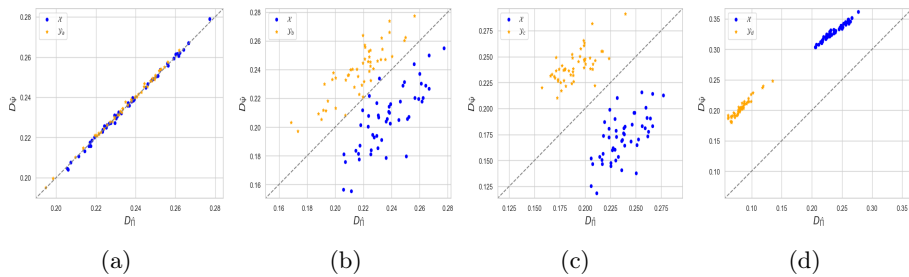
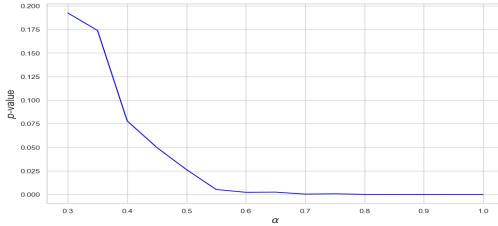


Fig. 6: Markovian DD-plots for ARCH(1) with parameters described in Table 3.

the distribution of two Markov chains. To do this, we will use the depth-based Wilcoxon rank-sum test, proposed in [34]. Consider two ARCH(1) models, one with $m(x) = (1 + \exp(-x))^{-1}$ and $\sigma(x) = \psi(x + 1.2) + 1.5\psi(x - 1.2)$, and the other with $m(x) = (1 + \alpha + \exp(-x))^{-1}$ and the same σ as the first one. For different values of α , ranging from 0.3 (very similar distributions) to 1 (reasonably different) we perform the aforementioned depth-based Wilcoxon rank-sum test, generating 50 trajectories of random length (between 50 and 200) for each chain and using a reference trajectory of length 1000 from the first chain. Figure 7 presents the p -values of the test for each α , averaged over 50 repetitions. The p -values effectively identify the differences between the two distributions when they exist.

Fig. 7: Average p -values (as a function of α) for the homogeneity test.